

Simultaneous material selection and geometry design of statically determinate trusses using continuous optimization

Sourav Rakshit · G. K. Ananthasuresh

Received: 6 June 2006 / Revised: 28 December 2006 / Published online: 5 April 2007
© Springer-Verlag 2007

Abstract In this work, we explore simultaneous geometry design and material selection for statically determinate trusses by posing it as a continuous optimization problem. The underlying principles of our approach are structural optimization and Ashby's procedure for material selection from a database. For simplicity and ease of initial implementation, only static loads are considered in this work with the intent of maximum stiffness, minimum weight/cost, and safety against failure. Safety of tensile and compression members in the truss is treated differently to prevent yield and buckling failures, respectively. Geometry variables such as lengths and orientations of members are taken to be the design variables in an assumed layout. Areas of cross-section of the members are determined to satisfy the failure constraints in each member. Along the lines of Ashby's material indices, a new design index is derived for trusses. The design index helps in choosing the most suitable material for any geometry of the truss. Using the design index, both the design space and the material database are searched simultaneously using gradient-based optimization algorithms. The important feature of our approach is that the formulated optimization problem is continuous, although the material selection from a database is an inherently discrete problem. A few illustrative examples are included. It is observed that the method is capable of determining the optimal topology in addition to optimal geometry when the assumed layout contains more links than are necessary for optimality.

Keywords Material selection · Geometry optimization · Failure criteria · Buckling · Truss design

List of symbols

E	Young's modulus
L	length of a truss member
ρ	mass density
M	material index
m	mass
P	internal force in a truss member
A	cross-section area of a truss member
S_t	tensile failure strength
ψ	composite geometry and function index
D	design index=ratio of ψ s for compressive and tensile members
SE	strain energy
K	global stiffness matrix
s	smoothing parameter
x	geometric design variable
\mathbf{u}	displacement vector
\mathbf{F}	external force vector
\mathbf{P}	internal force vector consisting of internal forces of all members
θ	angle of inclination of a member
\mathbf{R}	rotation matrix of a member in the truss structure
N_n	total number of nodes (vertices) in a truss
N_e	total number of members in a truss

List of subscripts

i	i^{th} member
t	tensile (member or load)
c	compressive (member or load)
i_1	first node in i^{th} member

S. Rakshit (✉) · G. K. Ananthasuresh
Mechanical Engineering Department,
Indian Institute of Science,
Bangalore 560012, India
e-mail: srakshit@mecheng.iisc.ernet.in

G. K. Ananthasuresh
e-mail: suresh@mecheng.iisc.ernet.in

- i_2 second node in i^{th} member
 l local coordinate system
 g global coordinate system

1 Introduction

Design of structures entails choosing the best material(s) and determining the optimal geometry. Structural designers either assume a material before optimizing the geometry or select the best material for an existing geometry of a structure. Either approach does not guarantee the optimal combination of geometry and material. Therefore, designers ought to consider geometry optimization and material selection simultaneously. However, this issue has been rarely addressed in the literature. In this paper, we present a framework for simultaneously optimizing the geometry and choosing the best material for statically determinate truss structures. This is a first step towards the development of a general method for a variety of structures. The novelty of our formulation is posing the inherently discrete problem of material selection as a continuous optimization problem and combining it with the geometry optimization. A brief description of the related work follows to bring out the differences and similarities between our approach and those of the past.

Size, shape, and topology optimization procedures are the three classes of extensively studied structural design methodologies with known or assumed material (Haftka and Gurdal 1994; Bendsoe and Sigmund 2003; Ananthasuresh 2003). The topology optimization methods have also been used to determine a microstructure for desired material properties by Sigmund (1994), Gibiansky and Sigmund (2000), and others. Simultaneous determination of the microstructure of the material, as well as the topology of a structure, has also been pursued (Turteltaub 2002; Bendsoe et al. 1994; Rodrigues et al. 2002; Guedes et al. 2005). In these methods, in addition to the topology variables, the parameters in the constitutive stress–strain relationship are taken as the design variables in the optimization problem. They have the advantage that different optimal material properties at each point in the optimized topology are determined. But they also have the disadvantage that a material with such optimized properties may or may not exist in reality. Furthermore, having different microstructures for different parts of the structure (i.e., inhomogeneous material distribution) is neither practical nor economical with the current state of manufacturing. Some practically viable methods have been proposed to choose the optimal orientation of lay-ups in different layers of composite shells by Stegmann and Lund (2005). Alternatively, when it is possible to justify the increased cost of

manufacturing, modern layered manufacturing methods may be used to realize optimal geometries with optimized inhomogeneous material microstructure (Dutta et al. 2001).

In the present work, we have neither defined a microstructure nor formed a constitutive material property relationship that is optimized. Instead, we choose from existing database of materials using Ashby's approach of material indices. Ashby's approach, as described in his book (Ashby 1999), helps choose the most suitable material when the geometry and loading of a component are known. To facilitate simultaneous optimization of the geometry and material selection, a design index was introduced by Ananthasuresh and Ashby (2003) in such a way that there exists a best material in the material database for every value of the design index. The design index depends on the geometry and functional requirements and, thus, serves as the coupling parameter in the simultaneous search of geometry and material spaces.

The design of statically determinate trusses is considered in this work to develop a framework for combining geometry optimization with the selection of the best material from a database. We use stiffness, strength, and cost/weight as the criteria for truss design.

Optimal design of trusses is a widely researched topic (Rozvany et al. 1995). The ground structure approach for truss design preceded the topology optimization by at least two decades. It is reported that the minimum weight design of trusses subject to stress constraints was considered by Dorn in 1964 (Achtziger 1996). Dorn had assumed that the allowable stresses in tensile and compression members are equal and showed that it can be posed as a linear programming problem. Achtziger (1996) proved that this can be done even when the two allowable stresses are different. Dorn, Achtziger (1996), Rozvany and Birker (1994), and others used the areas of cross-sections as the design variables. Recently, Stolpe and Svanberg (2004) included additional variables to select a different suitable material for each truss member from among a finite number of materials. They proved that at most two materials are sufficient in an optimal truss. They considered strength considerations as constraints in the optimization problem. Furthermore, they used yield stress as the limit even for compression members. But most often, slender compression members fail by buckling before their yield under compression occurs. Therefore, in this work, we consider buckling failure for compression members and yield failure for tensile members. An additional difference is that we do not pose the strength considerations as constraints but use them directly to determine the areas of cross-section. Thus, the design variables in the optimization problem are lengths and orientations (i.e., the geometry variables) of the truss members in an assumed layout. Achtziger (2005) has also solved the ground structure problem using geometry-

defining parameters as design variables. But in addition to these, he has taken the areas of cross-section as the design variables; that is not so in our case as mentioned above.

A few more points need to be noted about the approach taken in this paper. From the viewpoint of economical manufacturing and to avoid problems (e.g., galvanic corrosion) associated with two-material trusses, we insist on choosing a single best material for the optimal truss rather than two. Thus, this work differs from that of Stolpe and Svanberg (2004) who also considered material selection based on stress constraints. As stated earlier, we consider only available real materials in a database. Furthermore, although our approach does not explicitly address topology optimization, when some areas of cross-section go to the lower limit of zero (a small positive value in practice), the optimal topology may be different from the assumed initial layout.

The remaining four sections of this paper contain the following: a description of the design index and how it can be used to select the best material(s); the procedure for designing the geometry in conjunction with material selection; results, discussion, and possible future extensions; and finally, the concluding remarks.

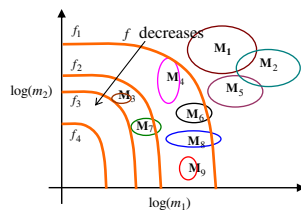
2 Selecting materials based on a design index

Our method of simultaneously designing the geometry and selecting the material, as noted above, is an extension of Ashby’s method of material selection (Ashby 1999). In Ashby’s method, when the objective f can be expressed as a separable function of functional requirements F , geometry G , and material properties M (i.e., $f = f_F(F)f_G(G)f_M(M)$ is possible); then, $f_M(M)$ is called a *material index*. This index helps choose the best material(s) from a database for the given $f_F(F)$ and $f_G(G)$. Instead of the above separable form, when f has the following form, the best material is chosen as described next.

$$f = D(F, G)m_1(M) + m_2(M) \tag{1}$$

For the purpose of illustration, Fig. 1 schematically shows an Ashby’s material selection chart with nine materials $\{M_1 \dots M_9\}$ for two material indices m_1 and m_2 on a log–log scale. A log–log scale is preferred in this chart because properties of all available materials differ by

Fig. 1 Material selection chart for two material indices, m_1 and m_2 , for a given value of $D(F, G)$ as per (1)



several orders of magnitude. The major and minor axes of the ovals in the figure indicate the range of values of the respective material indices of the corresponding materials. The figure also shows constant f curves for four different values of $f = \{f_1, f_2, f_3, f_4\}$ for a chosen value of $D(F, G)$ based on (1). Because f is constant along the curve, all the materials whose ovals overlap with it are equally good. Fixing the value of $D(F, G)$ implies that the geometry and functional requirements remain constant. Now, from the chart, we can see that the best available material(s) that minimize(s) the objective function f are M_3 and M_7 with a value of f_3 . There are no materials with a lower value of f in this example. Thus, for each $D(F, G)$, there exist one or more best materials. If we think of $D(F, G)$ as a *design index* (Ananthasuresh and Ashby 2003), which entirely depends on the geometry for given functional requirements, we are, thus, able to select the best material for that design.

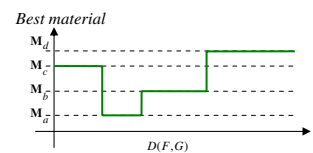
When the value of $D(F, G)$ changes, the shape of the constant f curve changes. Consequently, the best material(s) choice for minimum f would also change. By repeating the above procedure for different numerical values of $D(F, G)$, we can get the best material(s) for a desired range of $D(F, G)$. This is shown in Fig. 2. As can be seen in the figure, the choice of the best material usually remains the same for a finite range of values of $D(F, G)$. As noted above, for some range(s) of $D(F, G)$, more than one material may emerge as the best material. In those cases, it is immaterial which one of those is selected because they all give the same optimum value of the objective, f . We have used Cambridge Engineering Selector (CES, Cambridge Engineering Selector software, Granta design 2006, Cambridge, UK; <http://www.ces.com>) to cover the entire range of $D(F, G)$, i.e., $[0, \infty)$.

Based on the above approach of choosing the best material as a function of the design index, we formulate an optimization problem for simultaneously determining geometry and material for trusses. For this purpose, in the next section, we present the weight/cost objective with the strength requirement in truss design as shown in (1).

3 Functional requirements and design index for truss design

Every member in a truss experiences either tension or compression. The members under tension will fail by yielding, while those under compression are most likely to

Fig. 2 Best material vs design index



fail by buckling. In general, one best material exists for tension members and another for compression members. This intuitive observation was rigorously proved by Stolpe and Svanberg (2004). As noted earlier, we favor a single-material truss for reasons of economy, ease of manufacturing and assembly, and durability. Keeping this in mind, we present a design index next.

Let S_t be the permissible strength for a tensile member. Then, the area of cross-section A_t for a tensile member can be written as

$$A_t = P_t/S_t, \tag{2}$$

where P_t is the tension in the member. For compression members, buckling being the considered mode of failure, the area of cross-section for pin-ended truss members can be written for critical Euler buckling as follows:

$$A_c = \sqrt{\frac{\phi L_c^2 P_c}{\pi^2 E}}, \tag{3}$$

where L_c is the length of the member, P_c the compressive load, E the Young’s modulus, and ϕ the shape factor (Ashby 1999). For simplicity, we have considered a square cross-section for all truss members in our analysis. The mass of the whole truss can now be written as follows:

$$\begin{aligned} m &= \sum_{i=1}^{N_c} \rho A_i l_i + \sum_{i=1}^{N_t} \rho A_i l_i \\ &= \left\{ \sum_{i=1}^{N_c} \frac{L_{jc}}{\pi} \sqrt{12|P_{jc}|} \right\} \frac{\rho}{E^{1/2}} + \left\{ \sum_{i=1}^{N_t} (P_{ti} L_{ti}) \right\} \frac{\rho}{S_t}, \tag{4} \\ \Rightarrow m &= \{\psi_c\} \frac{\rho}{E^{1/2}} + \{\psi_t\} \frac{\rho}{S_t} \end{aligned}$$

where N_t and N_c are the number of members in tension and compression, respectively, and ρ , the mass density. For selecting the material to minimize the mass without loss of generality, (4) can be recast as (1).

$$\tilde{m} = \frac{\psi_c}{\psi_t} \frac{\rho}{E^{1/2}} + \frac{\rho}{S_t} = Dm_1 + m_2, \tag{5}$$

where $m_1 = \rho/S_t$ and $m_2 = \rho/E^{1/2}$ are material indices, and $D = \psi_c/\psi_t$ is the design index. Note that D is non-negative. Note also that (5) has the same form as (1).

The minimum weight objective is likely to give expensive or impractical materials to build trusses. Therefore, we consider the cost of material instead of weight as the objective. Then, the two material indices in (5) should be multiplied by the cost per unit mass of material. This is indicated as “price×material index” in the material selection

charts of Figs. 3 and 4 with the objective of the cost of material shown below:

$$cost = D(\text{price} \times m_1) + (\text{price} \times m_2). \tag{6}$$

The material selection chart in Fig. 3 was generated using the material database of only metals in the CES software (Cambridge Engineering Selector software, Granta design 2006, Cambridge, UK; <http://www.ces.com>; Ananthasuresh and Ashby 2003) and is reproduced in this study. Thus, Fig. 3 shows “price× ρ/S_t ” against “price× $\rho/E^{0.5}$ ” for only metals. In Fig. 3, the constant cost curves are shown for $D=0.01, 1,$ and 100 . Low alloy steels are the best choice until $D=1$. Cast iron dominates for values larger than one. This is expected because large values of D indicate that more members are under compression or that the compression loads are higher for both, of which cast iron is better than steel.

By creating another chart similar to the one in Fig. 3 for all engineering materials excluding polymers, the best choice of the material for the entire range of D was determined as shown in Fig. 4a and b.

The figures show two relevant material properties, viz., ρ and E , instead of indicating the name of the material as in Fig. 2. It is important to note that low alloy steel remains the best material for $0 \leq D \leq \sim 0.075$, and aerated concrete remains as the best material for $D \geq \sim 1.4$. Thus, we know the most suitable materials for the entire range of D . After this, we considered all polymers, and following similar steps as for the previous set of materials, we got the best choice of all polymer materials for the entire range of D as shown in Fig. 5a and b. In this case, polypropylene is the best material for $0 \leq D \leq \sim 0.1$, and phenol formaldehyde remains the best material for $D \geq \sim 3.5$. Thus, we know the most suitable polymer materials for the entire range of D .

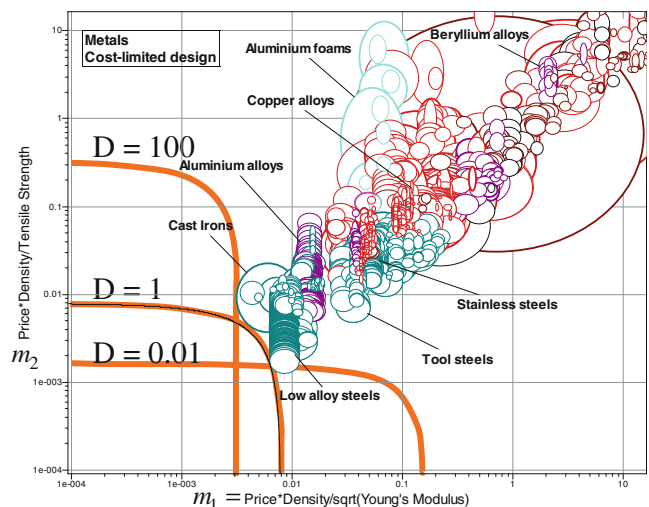
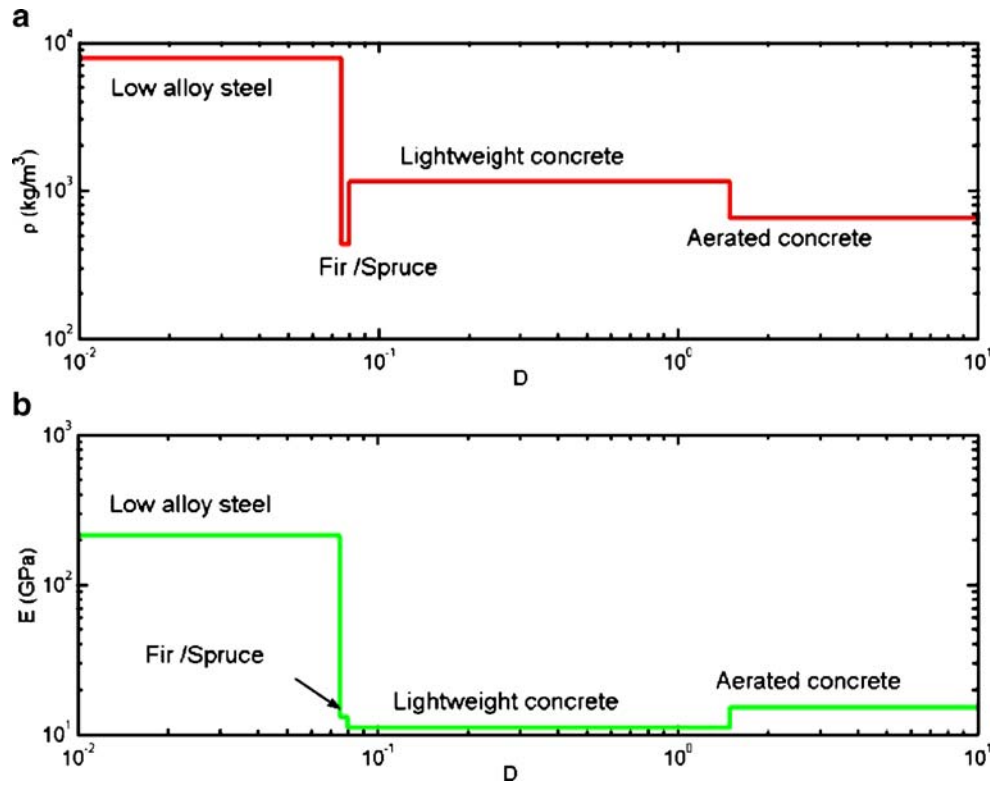


Fig. 3 Material selection for trusses considering only metals with price included. Low alloy steels and cast irons now emerge as the best candidates

Fig. 4 **a** Price ρ vs design index D for the best materials selected among all classes of engineering materials (except polymers). Mean values are shown instead of the min/max values. **b** Young's modulus E vs the design index D for the best materials selected among all classes of engineering materials (except polymers). The mean values are shown instead of the min/max values



4 Problem statement and solution procedure

Ananthasuresh and Ashby (2003) presented how materials can be selected based on failure criteria for a simple three-element truss (see Fig. 6) using the design index discussed

above. They showed that the design index D can be expressed as a function of the geometric parameter, θ , which is the angle that each inclined truss member makes with the base member. Because there is now an additional design freedom (namely θ), it is possible to optimize

Fig. 5 **a, b** Properties relevant to stiffness optimization from the best polymer materials selected for each value of D . The mean values are shown instead of the min/max values for each property

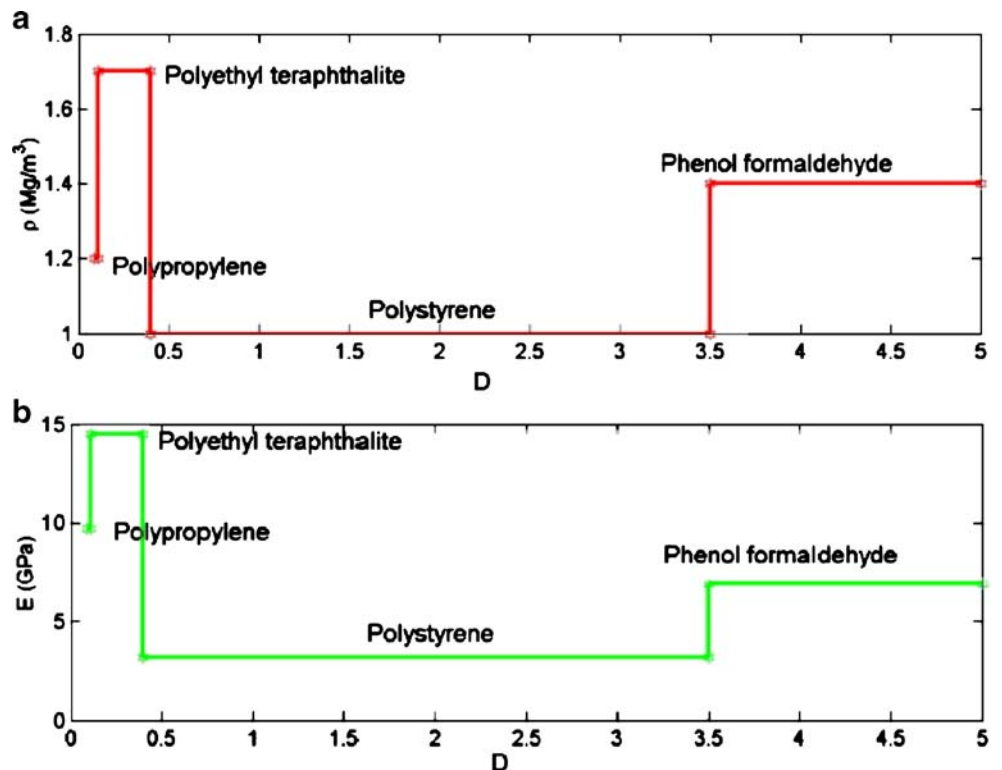
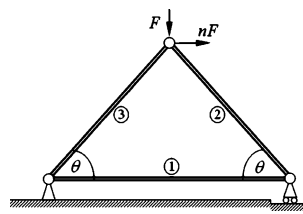


Fig. 6 Schematic of the simple truss (Ananthasuresh and Ashby 2003)



another functional requirement in addition to minimizing the cost. In this work, we extend their work by investigating how the design index would change when we consider trusses having more elements.

Just as in the case of the simple truss in Fig. 6, we take the geometry variables as the design variables in optimization. This is necessary because the areas of cross-section are determined by failure criteria, and thus, they are no longer the design variables. The internal forces on which the design index D depends are determined by the finite element analysis. This helps us choose the best material as per Fig. 4 or 5. The solution procedure is illustrated in Fig. 7 using a flowchart and is explained next.

Our objective is to determine the geometry of a truss subject to given static loads, boundary conditions on the

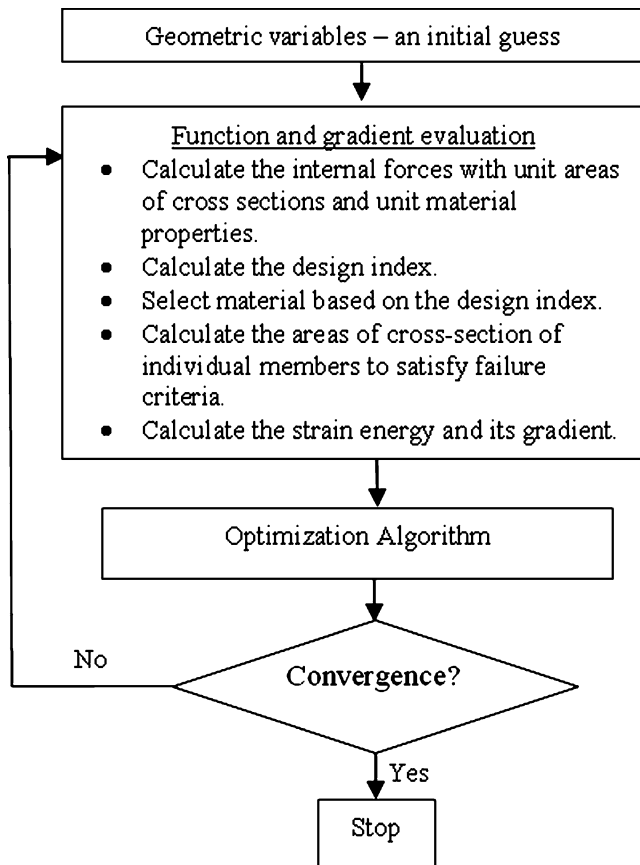


Fig. 7 Solution procedure for simultaneous material selection and geometry optimization of statically determinate structures

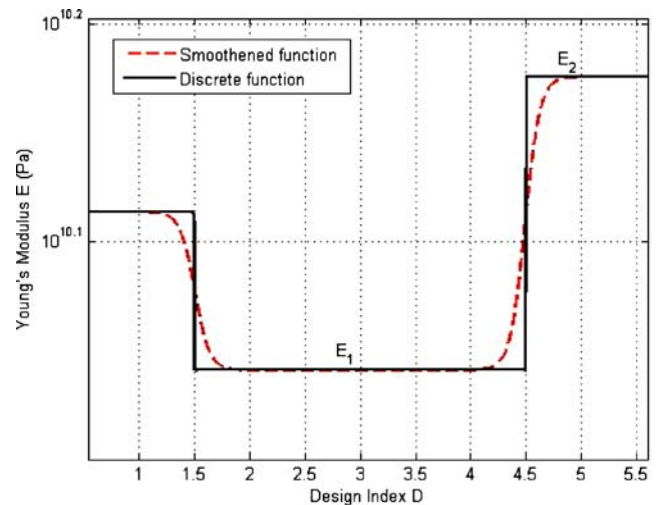


Fig. 8 The dashed line shows how, by using a sigmoid function, the discontinuous material property curve is made continuous

joints, and the size of the design domain. The requirements are maximum stiffness (minimum strain energy), minimum cost of material used, and safety against failure. The design variables are the lengths and the orientations of some of the elements that decide the overall geometry. For instance, in Fig. 9 of the first example, the length and orientation of element 1 are the geometry variables because of symmetry and the given fixed and force application points. The state variables are the areas of cross-section, displacements, internal forces of the members, and material properties. It should be noted that safety against failure determines the areas of the cross-section of the truss members. The selection of the best material is based on minimizing the cost of the material. The maximum stiffness requirement is met by optimizing over the design variables. The problem is posed as follows:

$$\text{Minimize: Strain energy} = \frac{1}{2} \mathbf{u}^T \mathbf{K} \mathbf{u} \tag{P1}$$

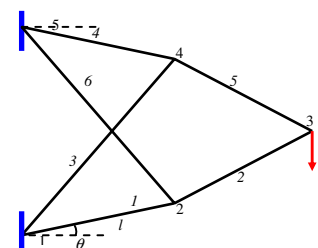
$$\text{Subject to: the static elastic equilibrium equation} \\ \mathbf{K} \mathbf{u} = \mathbf{F}$$

satisfying

$$u_j = 0 \text{ for degrees of freedom } j$$

$$F_k = F_{\text{external}} \text{ for specified degrees of freedom } k$$

Fig. 9 Example 1, l and θ are the design variables. The numerical labels of the truss members are indicated in italics



and failure criteria for tensile and compressive members, i.e.,

$$P_t = S_t A_t \tag{7}$$

$$P_c = \frac{\pi^2 E A_c^2}{\phi L_c^2} \tag{8}$$

It should be noticed that the failure criteria are not posed as constraints. Because the minimization of material cost is accomplished in selecting a material, that too is not posed as a constraint. However, if we want to put an upper bound on the material cost, it may be imposed as a constraint. The solution procedure is indicated in Fig. 7. The function evaluation for computing the strain energy is not straightforward in this study because the material is not known until the design index is computed. But the design index cannot be computed without knowing the internal forces in the trusses. Internal forces are to be computed by finite element analysis. For this, we need to know the areas of cross-section. But, areas of cross-section can be computed to satisfy the failure criteria only after we know the material and internal forces. This conflict is resolved for statically determinate trusses where the areas of cross-section and the material properties do not influence the internal forces for the given geometry and boundary conditions (i.e., loading and displacement boundary conditions). Henceforth, we continue with the description of the solution methodology for this class of trusses.

Because areas of cross-section and material properties do not influence the internal forces for the classes of trusses considered in this paper, we first take unit values for both and perform a finite element analysis to compute the internal forces. Then, the design index is evaluated. Based on this, the material is selected as per Fig. 4 or 5. By knowing the material properties and internal forces, we then compute the areas of cross-section using (2) and (3) to satisfy the respective failure criteria on tensile and compression members. After this, the finite element analysis is repeated with the chosen material and the computed areas of cross-section to evaluate the strain energy.

The selection of the material using Fig. 4 or 5 may imply a look-up table technique. Although it can be done that way, we do not adopt the look-up table method, as that would make the problem non-smooth. Instead, we smoothen the “material selection curve” in terms of a continuous value of the design index. This is discussed next.

4.1 Dealing with non-smoothness

Non-smoothness occurs in this problem when the design index changes the material choice abruptly as shown in Figs. 4 and 5. This poses a problem in calculating the

analytical derivatives of the material properties required in continuous optimization. We remove this by smoothening the curve at material transitions by using sigmoid function. This is illustrated in Fig. 8 with exaggerated smoothening for the sake of illustration. Mathematically, it can be written for Young’s modulus (and similarly for other properties) as follows:

$$E = E_1 + \sum_{i=2}^{N_m} \frac{E_i - E_{i-1}}{1 - e^{-s(D-D_{i-1})}}, \tag{9}$$

where N_m is the number of best materials over the entire range of D ; D_j , the j^{th} transition in the best material along the D -axis in Fig. 8; and s , the smoothening parameter. The above smoothening of the material property vs the design index curves is also realistic because all material properties always have a range of values. In generating Figs. 4 and 5, the average values within that range were considered. With smoothened model, the values will be anywhere within the range. Note, however, that the material properties are non-convex functions of the design index that, in turn, is a complicated function of the design variables. This makes the optimization problem (P1) non-convex.

4.2 Sensitivity analysis

We used the `fmincon` program of the Matlab (2006) toolbox to solve the optimization problem (P1). The gradients were computed analytically as explained next. The sensitivity analysis is somewhat intricate because the choice of material depends on the design variables. It is further complicated because strength related constraints (which determine the areas of cross-section) depend on both the material choice and the internal forces. Our approach to sensitivity analysis is described next.

Let x be the design variable. If we denote the strain energy as SE, then we can write its derivative with respect to the design variable as shown below:

$$\begin{aligned} \frac{dSE}{dx} = & \frac{1}{2} \mathbf{u}^T \left(\frac{\partial \mathbf{K}}{\partial x} + \frac{\partial \mathbf{K}}{\partial E} \frac{dE}{dx} + \frac{\partial \mathbf{K}}{\partial A} \frac{dA}{dx} \right) \mathbf{u} \\ & + \mathbf{u}^T \mathbf{K} \frac{d\mathbf{u}}{dx}. \end{aligned} \tag{10}$$

The symbols in the above equation are all defined at the beginning of the paper. The partial derivatives $\partial \mathbf{K} / \partial x$, $\partial \mathbf{K} / \partial E$ and $\partial \mathbf{K} / \partial A$ can easily be computed as we know the explicit dependence of the stiffness matrix \mathbf{K} on these quantities. The derivative of the Young’s modulus E is to be computed as follows:

$$\frac{dE}{dx} = \left(\frac{\partial E}{\partial D} \right) \left(\frac{dD}{dx} \right). \tag{11}$$

The first term in the right hand side of (11) is easily done with the help of (9). The computation of the second term is explained below:

$$\frac{dD}{dx} = \frac{\psi_t \frac{d\psi_c}{dx} - \psi_c \frac{d\psi_t}{dx}}{\psi_t^2}, \tag{12}$$

where

$$\frac{d\psi_t}{dx} = \sum_{i=1}^{N_t} \left(P_{t_i} \frac{dL_i}{dx} + L_i \frac{dP_{t_i}}{dx} \right), \tag{13}$$

$$\frac{d\psi_c}{dx} = \sum_{i=1}^{N_c} \frac{\sqrt{12}}{\pi} \left(2\sqrt{P_{c_i}} \frac{dL_i}{dx} + \frac{L_i^2}{2\sqrt{P_{c_i}}} \frac{dP_{c_i}}{dx} \right), \tag{14}$$

and N_t and N_c are the number of truss members in tension and compression, respectively.

By substituting (13) and (14) into (12), we get dD/dx , which we substitute back into (11) to get the material property derivative, dE/dx .

Next, we discuss how dA/dx is computed. For tensile and compression members, we get the following with the help of (2) and (3).

$$\frac{dA_i}{dx} = \frac{dS_t}{dx} P_{t_i} + S_t \frac{dP_{t_i}}{dx} \tag{15a}$$

$$\frac{dA_i}{dx} = \sqrt{12\pi} \left\{ \sqrt{\frac{P_{c_i}}{E}} \frac{dL_{c_i}}{dx} + \frac{L_{c_i}}{2\sqrt{EP_{c_i}}} \frac{dP_{c_i}}{dx} - \frac{L_{c_i}\sqrt{P_{c_i}}}{2E^{1.5}} \frac{dE}{dx} \right\} \tag{15b}$$

The two equations (15a and b) have the following general form.

$$\frac{dA_i}{dx} = \frac{\partial f}{\partial x} + \frac{\partial f}{\partial P_i} \frac{dP_i}{dx}, \tag{16}$$

where $A_i=f(x, P_i)$, i.e., some function of x and P_i .

It should be noticed that dA/dx involves components of dP/dx , which is not readily available. It can be computed from the element-level force equilibrium equations. That is, for individual members, in terms of local nodal displacement variables ($\mathbf{u}_{i_1}, \mathbf{u}_{i_2}$), we have

$$\frac{EA_i}{L_i} (\mathbf{u}_{i_1} - \mathbf{u}_{i_2}) = P_i, \tag{17}$$

the differentiation of which yields

$$\begin{aligned} \frac{dE}{dx} \frac{A_i}{L_i} (\mathbf{u}_{i_1} - \mathbf{u}_{i_2}) + \frac{dA_i}{dx} \frac{E}{L_i} (\mathbf{u}_{i_1} - \mathbf{u}_{i_2}) - \frac{EA_i}{L_i^2} \frac{dL_i}{dx} (\mathbf{u}_{i_1} - \mathbf{u}_{i_2}) \\ + \frac{EA_i}{L_i} \left(\frac{d\mathbf{u}_{i_1}}{dx} - \frac{d\mathbf{u}_{i_2}}{dx} \right) = \frac{dP_i}{dx} \\ \Rightarrow \frac{P_i}{E} \frac{dE}{dx} + \frac{P_i}{A_i} \frac{dA_i}{dx} - \frac{P_i}{L_i} \frac{dL_i}{dx} + \frac{EA_i}{L_i} \left(\frac{d\mathbf{u}_{i_1}}{dx} - \frac{d\mathbf{u}_{i_2}}{dx} \right) = \frac{dP_i}{dx}. \end{aligned} \tag{18}$$

By noting the coordinate transformation $\mathbf{u}_{i_1} = R\mathbf{u}_{g_i}$ between the local (i.e., \mathbf{u}_{i_1}) and global (i.e., \mathbf{u}_{g_i}) displacement variables for the i^{th} element, we obtain

$$\frac{d\mathbf{u}_{i_1}}{dx} - \frac{d\mathbf{u}_{i_2}}{dx} = \mathbf{b} \frac{d\mathbf{u}_{g_i}}{dx} + \frac{d\mathbf{b}}{dx} \mathbf{u}_{g_i}, \tag{19}$$

where $\mathbf{b} = [\cos(\theta_i) \sin(\theta_i) - \cos(\theta_i) - \sin(\theta_i)]$. The substitution of (19) into (18) yields

$$\frac{P_i}{E} \frac{dE}{dx} + \frac{P_i}{A_i} \frac{dA_i}{dx} - \frac{P_i}{L_i} \frac{dL_i}{dx} + \frac{EA_i}{L_i} \left(\mathbf{b} \frac{d\mathbf{u}_{g_i}}{dx} + \frac{d\mathbf{b}}{dx} \mathbf{u}_{g_i} \right) = \frac{dP_i}{dx}. \tag{20}$$

When this operation is done for all the N_e elements, (20) gives

$$[\mathbf{C} \mathbf{B}] \left\{ \frac{d\mathbf{P}}{dx} \right\} = \{\mathbf{g}\}, \tag{21}$$

where \mathbf{C} , \mathbf{B} and \mathbf{g} are the collective expressions making up the coefficients of $\frac{dP}{dx}$, $\frac{d\mathbf{u}}{dx}$, and unity, respectively. But this now involves $d\mathbf{u}/dx$. Both dP/dx and $d\mathbf{u}/dx$ also appear in additional $2N_n$ equations that are obtained by differentiating the global force equilibrium equation.

$$\begin{aligned} \mathbf{K}\mathbf{u} &= \mathbf{F} \\ \Rightarrow \left(\frac{\partial \mathbf{K}}{\partial x} + \frac{\partial \mathbf{K}}{\partial E} \frac{dE}{dx} + \frac{\partial \mathbf{K}}{\partial A} \frac{dA}{dx} \right) \mathbf{u} + \mathbf{K} \frac{d\mathbf{u}}{dx} &= 0 \\ \Rightarrow \left\{ \frac{\partial \mathbf{K}}{\partial x} + \frac{\partial \mathbf{K}}{\partial E} \frac{dE}{dD} \frac{dD}{dP} \frac{dP}{dx} + \frac{\partial \mathbf{K}}{\partial A} \left(\frac{\partial f}{\partial x} + \frac{\partial f}{\partial A} \frac{dP}{dx} \right) \right\} \mathbf{u} \\ + \mathbf{K} \frac{d\mathbf{u}}{dx} &= 0 \end{aligned} \tag{22}$$

Now, (21) and (22) together yield the (N_e+2N_n) equations in terms of equal number of variables, viz., dP/dx and $d\mathbf{u}/dx$, as shown below:

$$\begin{bmatrix} \mathbf{C} & \mathbf{B} \\ \mathbf{Q} & \mathbf{K} \end{bmatrix} \begin{bmatrix} \frac{d\mathbf{P}}{dx} \\ \frac{d\mathbf{u}}{dx} \end{bmatrix} = \begin{bmatrix} -\frac{\partial \mathbf{K}}{\partial x} \mathbf{u} - \frac{\mathbf{g}}{\partial x} \frac{\partial \mathbf{K}}{\partial A} \mathbf{u} \end{bmatrix}, \tag{23}$$

where $\mathbf{Q} = \frac{dE}{dD} \frac{dD}{dP} \frac{\partial \mathbf{K}}{\partial E} \mathbf{u} + \frac{\partial f}{\partial A} \frac{\partial \mathbf{K}}{\partial A} \mathbf{u}$. By solving (23), all other quantities pertaining to the sensitivity of the strain energy can now be computed.

The results of finite difference derivatives and analytical derivative calculated by our method for example 1 for a load of 1,000 N are as follows:

- Results from finite difference derivative= $[-1.141 \ 5.4573]$,
- Results from analytical calculation= $[-1.141 \ 5.4573]$,
- Difference= $[0.2855 \ 0.5255] \times 10^{-4}$, and
- Percentage error= $[25.022 \ 9.6284] \times 10^{-6}$.

Next, we show some results to illustrate how, depending on the loading conditions, boundaries and size, different

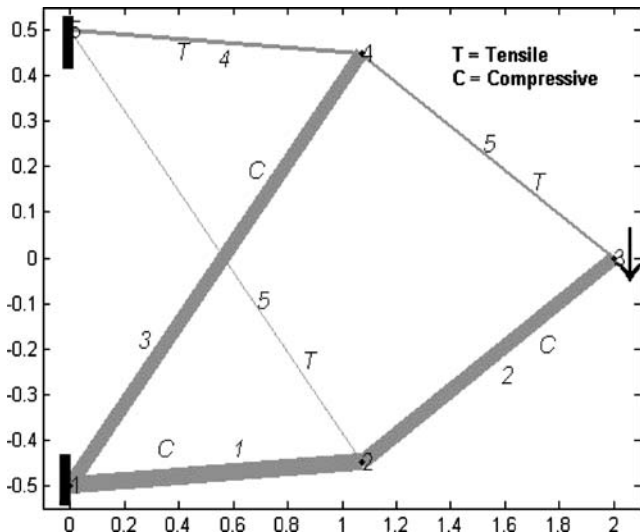


Fig. 10 Optimal layout of the structure shown in Fig. 9 for force=1,000 N. The selected best material is low alloy steel. The material cost of the truss is \$1.287. The strain energy calculated is 18.7325 J

materials are selected as the single best material for the entire truss along with, of course, the best geometry and areas of cross-section for individual members.

5 Results and discussion

5.1 Example 1

For the first example, the topology, loads, and the displacement boundary conditions are taken as shown in Fig. 9. Nodes 1 and 5 are fixed. The length and inclination of element 1 are the geometry-defining design variables. Due to symmetry, the lengths of elements 1 and 4 are the same, and the inclination of element 4 is the mirror image of that of element 1 about the horizontal axis. A downward vertical force of 1,000 N is applied at node 3. The structure is 2 m long in the horizontal direction and 1 m in the vertical direction. For these specifications, the optimal geometry was obtained as shown in Fig. 10. The corresponding material was low alloy steel. The cross-sectional areas of the members in the increasing order of element numbers are $1.0e-003 \times [0.1004 \ 0.0839 \ 0.0871 \ 0.0007 \ 0.0005 \ 0.0003]$ m². The corresponding internal forces are $1.0e+003 \times [-1.52015 \ -1.151 \ -0.643 \ 1.52015 \ 1.151 \ 0.643]$ N. A positive sign indicates the tensile force, whereas a negative sign the compressive force. The value of the design index *D* for the optimum solution is 0.0392, and the cost of material is \$1.287.¹ The widths of the

¹ This does not include the cost of processing the material. Therefore, it only gives the cost of raw material as given in the database of CES software (Cambridge Engineering Selector software, Granta design 2003, Cambridge, UK; <http://www.ces.com>).

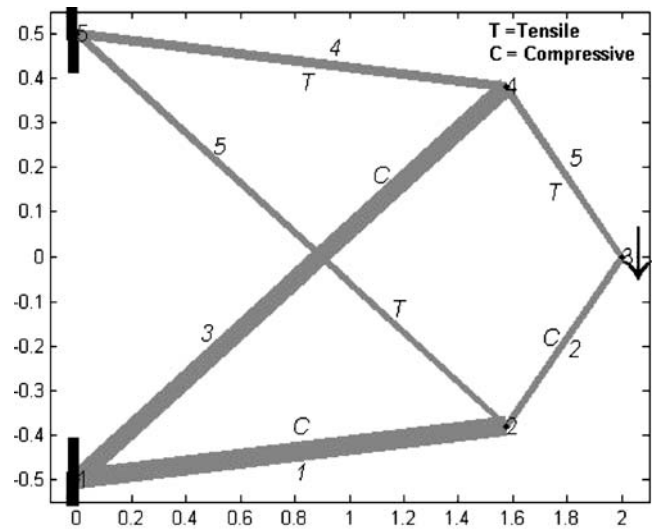


Fig. 11 The optimal layout for structure with force=90 N but with the same specifications as in Fig. 9. The best material is lightweight concrete. The cost of the material is \$0.0357. Strain energy is 0.034 J

members shown in all the figures are only representative and are not to scale. This is because some cross-section areas are more than 100 times larger than some others.

A few variations of this example were tried to see how the optimal geometry and the best material choice vary with different specifications. When the applied force was reduced to 90 N, keeping everything else the same, the best material turned out to be lightweight concrete. The corresponding optimized geometry is shown in Fig. 11. The areas of cross-section in the increasing order of element number were computed to be $1.0e-003 \times [0.1785 \ 0.0492 \ 0.1635 \ 0.0796 \ 0.0465 \ 0.0512]$ m². The corresponding internal forces are $1.0e+002 \times [-1.155 \ -0.675 \ -0.743 \ 1.155 \ 0.675 \ 0.743]$ N. The value of the design index *D* is

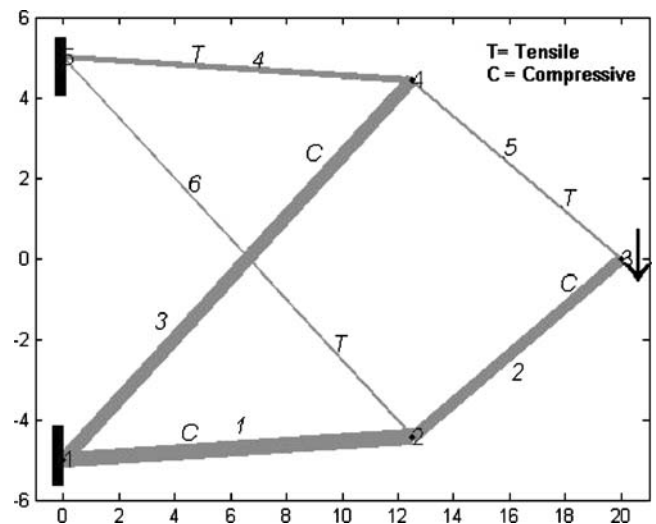


Fig. 12 Optimum geometry corresponding to a structure ten times as big as that of Fig. 9. The applied force *F*=1,000 N. The best material comes out to be lightweight concrete. The cost of the material is \$7.659, and the strain energy is 2.935 J

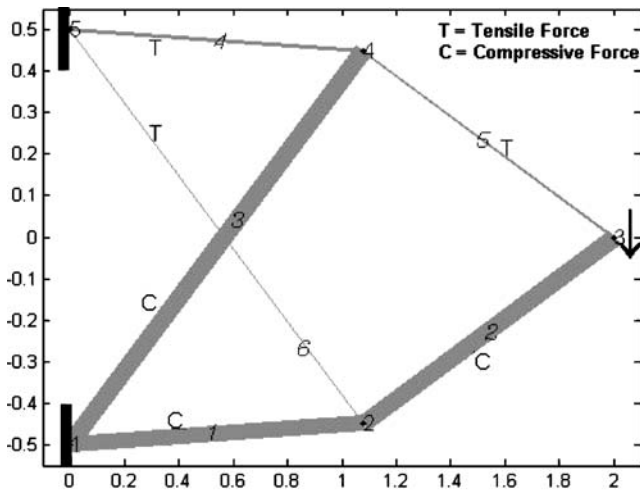


Fig. 13 Optimum polymer structure with force=100 N. The best material is polyethyl teraphthalite. The cost of the materials is \$0.0012, and the strain energy is 0.9 J

0.179. We see that, although the internal forces are less than those in the previous case, the cross-sectional areas are larger; this is because the material selected is lightweight concrete that has much lower failure strength and Young’s modulus than those of a low alloy steel. At first sight, this may appear counterintuitive, as larger value of cross-sectional areas mean higher volume of material, but the density×price of cast iron is much lower than that of steel. This is determined by the appropriate value of D .

When the size was increased by a factor of 10 (while keeping all others, including the force, the same), once again, lightweight concrete emerged as the best material. Its optimal geometry is shown in Fig. 12. For the same geometrical layout when polymers are considered instead of all engineering materials excluding polymers (see Fig. 5), polyethyl teraphthalite became the best material (Fig. 13).

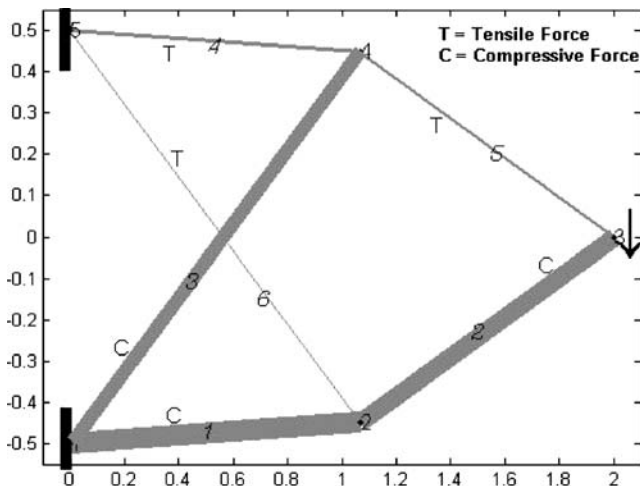
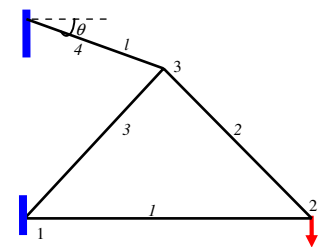


Fig. 14 Optimal layout for force=1,000 N, with polypropylene as the best material. The cost of the material is \$0.0024, and the strain energy is 405.063 J

Fig. 15 Example 2, l and θ are the design variables. The numerical labels of the truss members are indicated in *italics*



When the force was increased to 1,000 N, the best material was polypropylene (Figs. 14 and 15).

5.2 Example 2

The specifications for the second example are shown in Fig. 14. The design domain is 2 m long and 1 m in height. The applied external load is 1,000 N. The optimal material came out to be low alloy steel, and the optimal structure is shown in Fig. 16. Now we changed the load to 100 N. The optimal material turns out to be lightweight concrete, the optimal geometry of which is shown in Fig. 17.

We now consider a force of 1,000 N, which is directed along member 1. Only member 1 is adequate to withstand such an external load. For this case, we indeed got this result. The resulting structure is shown in Fig. 18. The cross-sectional areas of the elements in order of increasing element number are $1.0e-003 \times [0.5694 \ 0.0001 \ 0.0001 \ 0.0001]$ m². The corresponding internal forces in the elements were $1.0e+003 \times [1.0 \ 0.0 \ 0.0 \ 0.0]$ N. We notice that the cross-section areas for members 2, 3, and 4 have reached their lower bounds (this is indicated by dashed lines in the figure), and the corresponding internal forces in them are zero. Thus, we can safely omit all elements except element 1. This defines a new topology in the sense that,

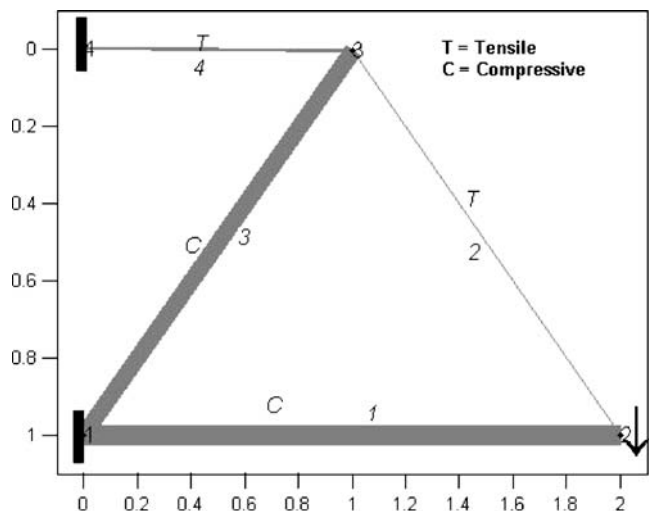


Fig. 16 Optimal layout for structure in Fig. 15 with force=1,000 N. The best single material is low alloy steel. The material cost is \$1.947, and the strain energy is 20.0125 J

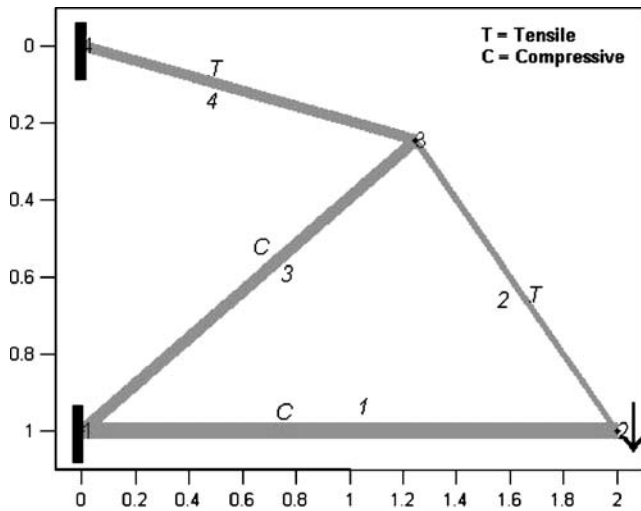


Fig. 17 The optimal structure for force=100 N and everything else is the same as in Fig. 15. The selected material is lightweight concrete. The material cost is \$0.0397, and the strain energy is 0.0368 J

instead of connectivity among four nodes {1, 2, 3, 4}, we now have the connectivity only between {1, 2}.

5.3 Example 3

The specifications for this example are shown in Fig. 19. The number of geometry design variables is four. For a load of 1,000 N, the optimum material turned out to be low alloy steel whose geometry is shown in Fig. 20. This solution resembles a structure with bars (compression members) and wires (tension members).

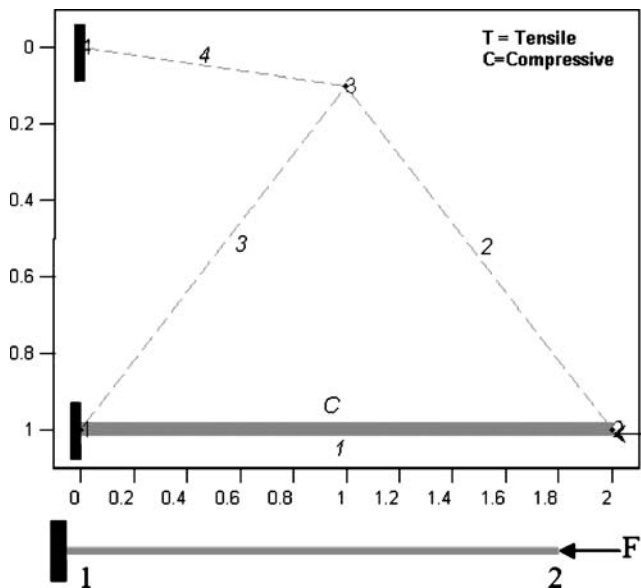
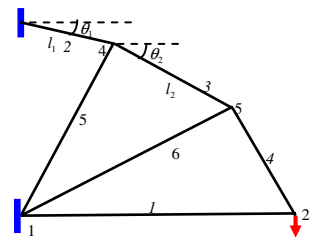


Fig. 18 The optimal structure when only a horizontal load=1,000 N is applied. The internal forces in the *dashed* members are zero, and their cross-sections have reached the lower limit. Hence, such members may be safely removed from the parent structure. The best material is aerated concrete. The material cost is \$0.0378, and the strain energy is 0.1171 J

Fig. 19 Example 3: $l_1, \theta_1, l_2,$ and θ_2 are the design variables. The numerical labels of the truss members are indicated in *italics*



5.4 Example 4

We now consider an example with a comparatively larger number of design variables. The geometry of the structure looks as shown in Fig. 21. A force of 100 N is applied. The best material turns out to be lightweight concrete. The optimal layout is shown in Fig. 22.

The cross-sectional areas of the members in the order of increasing element number are $1.0e-003 \times [0.0714 \ 0.0705 \ 0.0697 \ 0.0701 \ 0.0206 \ 0.0348 \ 0.0352 \ 0.0001 \ 0.0001 \ 0.1358 \ 0.1213 \ 0.1314]$ m², and the corresponding internal forces in the members are $[103.4863 \ 102.2319 \ 101.0751 \ 101.7031 \ -18.5343 \ -18.5343 \ 0.0 \ 0.0 \ -41.0978 \ -33.4393 \ -39.7630]$ N. We note that members 8 and 9 have reached the lower limit for cross-section areas. The corresponding internal forces are also zero. Therefore, we can safely eliminate these members without altering the forces in the other members of the structure. This will define a new topology for the structure, which is shown in Fig. 23.

6 Discussion

In the course of the optimization procedure, we noticed that it takes about the same number of iterations as the usual geometry optimization with a fixed material. This is shown in Table 1.

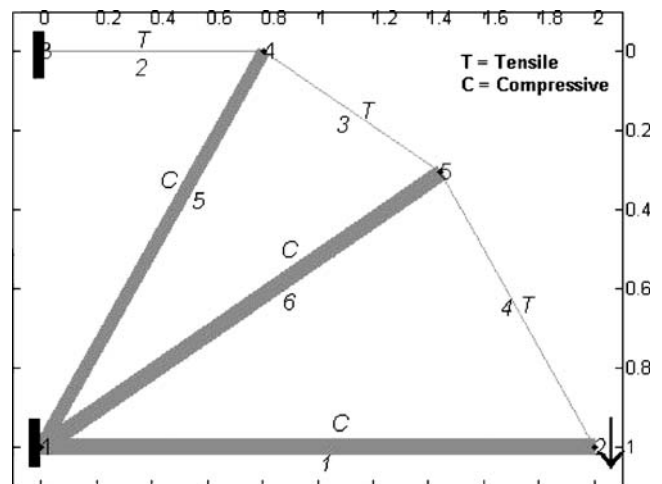


Fig. 20 The optimal layout for the structure in Fig. 17 and force=1,000 N. The best material is low alloy steel. The material cost is \$2.23, and the strain energy is 19.415 J

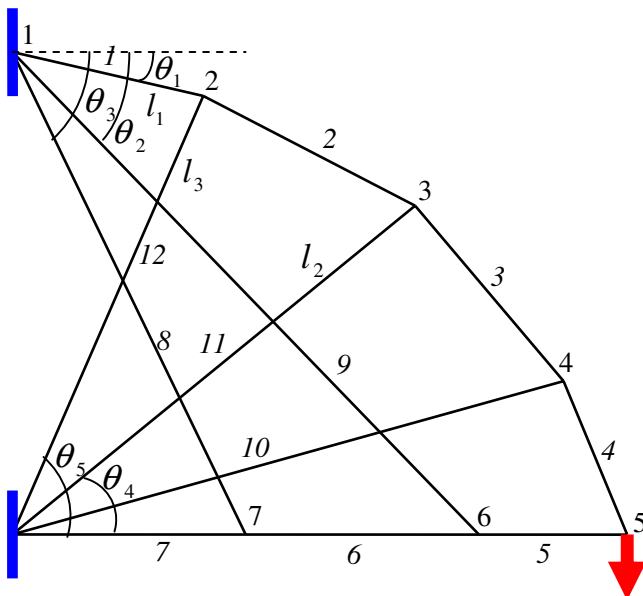


Fig. 21 Example 4: $l_1, \theta_1, l_2, \theta_2, l_3, \theta_3, \theta_4$, and θ_5 are the design variables. The numerical labels of the truss members are indicated in *italics*

Thus, the method described in this paper is a new way of reducing computation time for researchers who follow the procedure of taking each material from a prospective best-material set and optimizing the geometry and, finally, choosing the best combination of material and geometry.

It should be noted that some of the examples occasionally encountered convergence problems. This is to be expected because this problem is inherently non-smooth. Although the non-smoothness due to material selection is circumvented by smoothing, this does not ensure smoothness when a truss member suddenly changes from being tensile to compressive or vice versa as the geometry changes. It occurs rarely, and so it did not affect most of the examples attempted to generate the results for this work. In

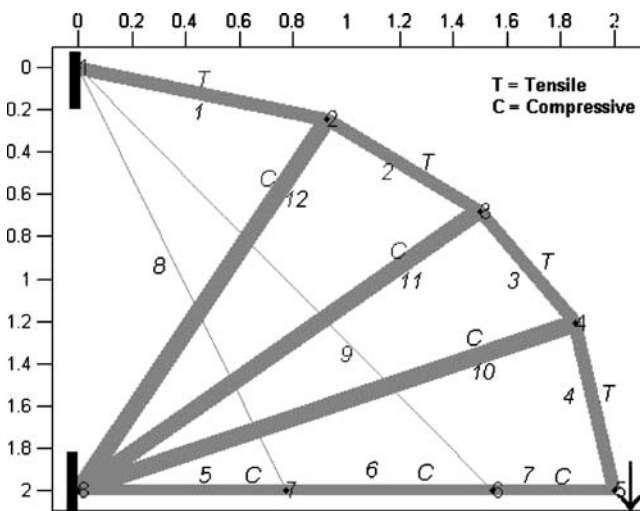
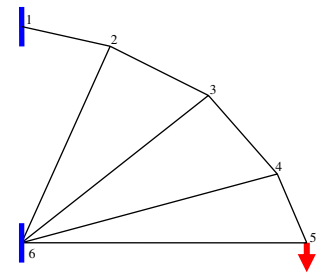


Fig. 22 The optimal layout for the structure in Fig. 20 and force = 100 N. The best material is lightweight concrete. The material cost is \$0.0445, and the strain energy is 0.0251 J

Fig. 23 The optimal topology after removing non-loaded members



our work, we selected the maximum and minimum bounds on the design variables so that the tensile members remain tensile and compressive members compressive, and strain energy is a smooth function of the design variables.

This can be illustrated with the first example for which the strain energy is plotted as a function of design variables L_1 and θ_1 for both restricted and unrestricted design domains in Figs. 24 and 25. It can be noticed that the differentiability of the strain energy is lost outside the design domain. This is due to the change of sign in the internal forces. This type of change in sign for a geometric parameter (θ_1 for example 1) is shown in Figs. 26 and 27.

In the methodology presented in this paper, we have selected only the statically determinate trusses, i.e., the trusses with zero *states of self-stress* (Calladine 1978). The number of states of self-stress implies that such a truss cannot be assembled without stressing at least that many members of truss. The states of self-stress can be determined by Maxwell’s rules as pointed out by Calladine (1978), or equivalently, using the Grubler’s formula (Erdman et al. 1984) for determining the degrees of freedom (*dof*) of a linkage. A number *dof* with the negative sign indicates the number of states of self-stress. For a planar truss structure, the Maxwell’s rule gives that if there are v vertices (nodes) in a truss, then the minimum number of members b required to satisfy the Maxwell’s rule is $b = 2v - 3$. The same result can be derived from Grubler’s formula for the number of *dof* for linkages. According to this, the number of *dof* of a linkage having b members and j single *dof* joints is given by $dof = 3(b - 1) - 2j$.

The current procedure described in this paper applies only to statically determinate trusses under a single loading condition. This can be justified on the basis of the fact that

Table 1 Number of function evaluations for example 1

Material	Number of function evaluations
Low alloy steel	21
Wood	22
Lightweight concrete	19
Aerated concrete	22
Simultaneous material selection and geometry optimization	21

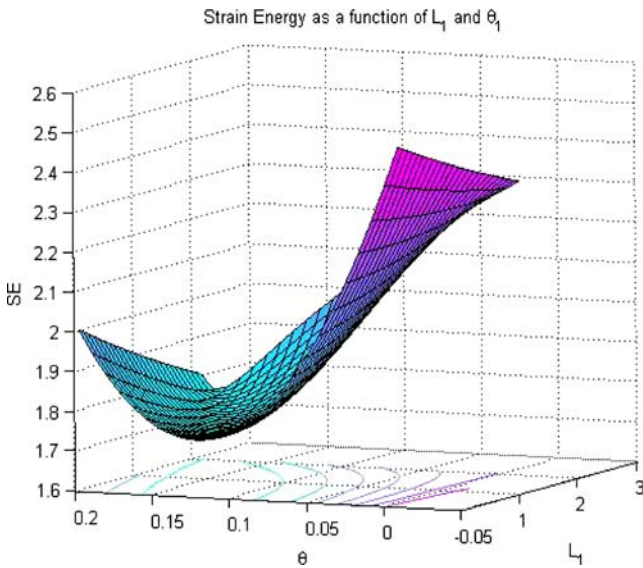


Fig. 24 The strain energy as a smooth function of design variables in the range $0 \leq L_1 \leq 2$ m and $0 \leq \theta_1 \leq 0.2$ rad. As seen, the function is smooth

optimal layouts of trusses are usually statically determinate. As Calladine (1978) noted, they are “simply stiff,” having states of zero self-stress and not ones that are “over-stiff” or “redundant” (statically indeterminate) that have states of self-stress less than zero. Because the number of states of self-stress implies that such a truss cannot be assembled without stressing at least that many members, it can be argued that a statically indeterminate truss will contain a larger number of stressed members than a statically determinate one for similar geometry, external loads, and boundary conditions. This will automatically rule out statically indeterminate truss layouts from our scope of optimization, as our objective is to minimize the strain energy. Special geometrical relationships and symmetry may enable the assembly of statically indeterminate trusses

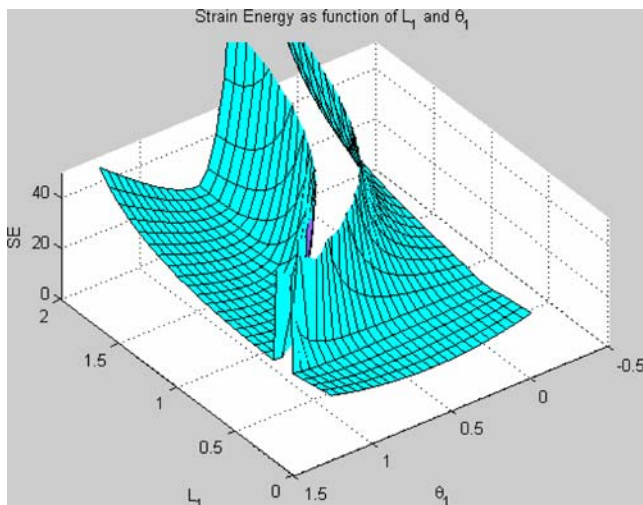


Fig. 25 The strain energy in the range $0 \leq L_1 \leq 2$ m and $0 \leq \theta_1 \leq \frac{\pi}{2}$ rad. As seen, the function is non-smooth. This occurs when there is transition from tensile to compressive members

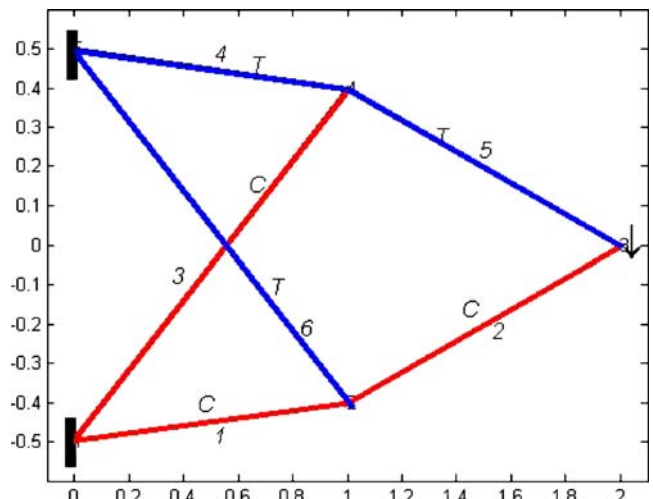


Fig. 26 Tensile and compressive members in the range $0 \leq L_1 \leq 2$ m and $0 \leq \theta_1 \leq 0.2$ rad. Tensile members are colored blue and the compressive members red

layouts without any stressed members. Hence, considering such layouts in the framework presented in this paper may have merit, and it is worth pursuing to see if such special geometrical relationships emerge from the geometry optimization. When multiple loading conditions are considered, a statically determinate truss may no longer be optimal. Therefore, a future extension of this work is to consider statically indeterminate trusses as well as other structures such as frames consisting of beam elements. For these types, a new method is needed for computing the design index.

In our work, we have not included the cost of processing the materials or the cost of joints between the truss members. This can be included in the formulation of the problem as a constraint. Ashby’s method of process selection will be useful in this regard. This forms the basis

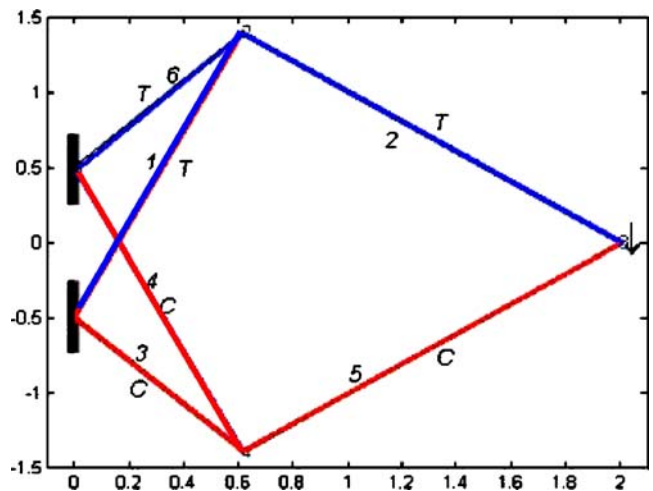


Fig. 27 Tensile and compressive members for a value of $\theta_1 \geq 0.2$ rad. Tensile members are colored blue and compressive members red. Notice that member 5 has become compressive and member 6 tensile. Such change in the direction of the internal force in the members give rise to non-convexity in strain energy

for broadening this work, which is a first step toward a more general method for more realistic scenarios.

7 Closure

This paper is concerned with simultaneous optimal selection of a material and determination of the geometry of statically determinate trusses under static loads. Most structural designers have to design with materials that are readily available in the market. This need has prompted us to deal with readily available materials rather than going for materials with tailor-made microstructures. Therefore, we consider the available materials in a database and used a design index to choose the best *single* material along with the corresponding best geometry. This methodology is developed with the simplest type of structures—trusses. An optimization problem is formulated to maximize the stiffness of a structure while simultaneously minimizing the cost of material and obeying failure criteria for tensile and compression members. Three examples and their variants are presented to illustrate the influence of the size and the magnitude of the force on the resulting optimum combinations of material and geometry. Two examples show that even the topology can change when some members reach their lower limit (almost zero) on the cross-section area. Thus, it shows the promise for posing and solving the most general problem of topology optimization with geometric variables and material selection from a database in a framework that allows the use of gradient-based continuous optimization algorithms. A few issues for further work are also identified.

Acknowledgment The second author thanks Prof. M. F. Ashby with whose collaboration this work was initiated and the concept of the design index was conceived.

References

- Achtziger W (1996) Truss topology optimization including properties different for tension and compression. *Struct Optim* 12:63–74
- Ananthasuresh GK (ed) (2003) *Optimal synthesis methods for MEMS*. Kluwer, Norwell, MA
- Ananthasuresh GK, Ashby MF (2003) Concurrent design and material selection for trusses. Proceedings of the workshop on optimal design Laboratoire de Mechanique des Solides Ecole Polytechnique Palaiseau, France, November 26–28, 2003
- Ashby MF (1999) *Materials selection in mechanical design*, 2nd edn. Butterworth Heinemann, New York
- Bendsoe, Sigmund (2003) *Topology optimization theory, methods and applications*, 2nd edn. Springer, Berlin Heidelberg New York
- Bendsoe MP, Guedes JM, Haber RB, Pedersen P, Taylor JE (1994) An analytical model to predict optimal material properties in the context of optimal structural design. *J Appl Mech* 61(4):930–937
- Calladine CR (1978) Buckminster Fuller's "tensegrity" structures and Clerk Maxwell's rules for and construction of stiff frames. *Int J Solids Struct* 14(2):161–172
- Dutta D, Prinz FB, Rosen D, Weiss L (2001) Layered manufacturing: current status and future trends. *J Comput Inf Sci Eng* 1:60–71
- Erdman AG, Sandor GN, Kota Sridhar (1984) *Mechanism design: analysis and synthesis*, vol. I, 4th edn. Prentice Hall, New York
- Gibiansky LV, Sigmund O (2000) Multiphase composites with extremal bulk modulus. *J Mech Phys Solids* 48:461–498
- Guedes JM, Bendsoe MP, Rodrigues H (2005) Hierarchical optimization of material and structure for thermal transient problems. In: Bendsoe MP, Olhoff N, Sigmund O (eds) *IUTAM Symposium, Rungstedgaard, Copenhagen, Denmark, (October 26–29, 2005)*, pp 309–318
- Haftka Gurdal (1994) *Principles of structural optimization*, 3rd edn. Kluwer, Norwell, MA
- Rodrigues H, Guedes JM, Bendsoe MP (2002) Hierarchical optimization of material and structure. *Struct Multidiscipl Optim* 24:1–10
- Rozvany GIN, Birker (1994) On singular topologies in exact layout optimization. *Struct Optim* 8:228–235
- Rozvany GIN, Bendsoe MP, Kirsch U (1995) Layout optimization of structures. *Appl Mech Rev* 48:41–119
- Sigmund O (1994) Materials with prescribed constitutive parameters: an inverse homogenization problem. *Int J Solids Struct* 31(17):2313–2329
- Stegmann Jan, Lund Erik (2005) On discrete material optimization of laminated composites using global and local criteria. In: Bendsoe O, Sigmund O (eds) *IUTAM symposium, Rungstedgaard, Copenhagen, Denmark, October 26–29, 2005*, pp 385–396
- Stolpe M, Svanberg K (2004) A stress-constrained truss-topology and material-selection problem that can be solved by linear programming. *Struct Multidiscipl Optim* 27:126–129
- Turteltaub S (2002) Optimal control and optimization of functionally graded materials for thermomechanical processes. *Int J Solids Struct* 39(12):3175–3197